Journal of Hazardous Materials 437 (2022) 129367

Contents lists available at ScienceDirect

Journal of Hazardous Materials

journal homepage: www.elsevier.com/locate/jhazmat

How sulfur species can accelerate the biological immobilization of the toxic selenium oxyanions and promote stable hexagonal Se^0 formation

B. Song, J. Weijma, C.J.N. Buisman, R.D. van der Weijden *

Department of Environmental Technology, Wageningen University and Research, the Netherlands

HIGHLIGHTS

- Sulfur species promote generation and recovery of a stable hexagonal Se^0 phase.
- The presence of bio-S^0 and SO_4^{2-} can increase the SeO_3^{2-} removal rate.
- SeS_2 bio-reduction induces a cycle of SeS_2 generation resulting in Se^0.

GRAPHICAL ABSTRACT

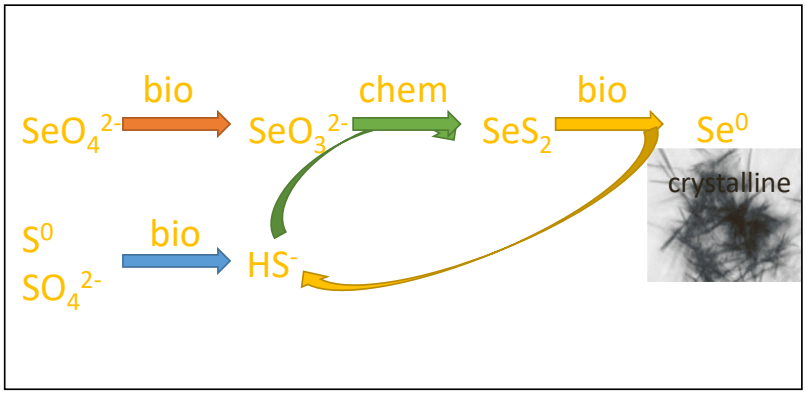

ARTICLE INFO

Editor: Dr. T Meiping

Keywords:
Hexagonal selenium
Bio-reduction
Sulfur bio-cycling
Selenium-sulfur

ABSTRACT

Toxic selenium oxyanions and sulfur species are often jointly present in contaminated waters and soils. This study investigated the effect on kinetics and resulting products for bio-reduction of selenium oxyanions in the presence of biologically produced sulfur resulting from bio-oxidation of sulfide in (bio)gas-desulfurization (bio-S^0) and of sulfate. Selenite and selenate (~2 mmol L^{-1}) bio-reduction was studied in batch up to 28 days at 30 °C and pH 7 using lactic acid and a sulfate-reducing sludge, 'Emmtec'. Bio-S^0 addition increased the selenite removal rate, but initially slightly decreased selenate reduction rates. Selenite reacted with biologically generated sulfide resulting in selenium-sulfur, which upon further bio-reduction creates a sulfur bio-reduction cycle. Sulfate addition increased the bio-reduction rate for both selenite and sulfate. Bio-S^0 or sulfate promoted hexagonal selenium formation, whereas without these, mostly amorphous Se^0 resulted. With another inoculum, 'Eerbeek', bio-S^0 accelerated the selenite reduction rate less than for 'Emmtec' because of lower sulfur and higher selenite bio-reduction rates. Bio-S^0 addition increased the selenate reduction rate slightly and accelerated hexagonal selenium formation. Hexagonal selenium formation is advantageous because it facilitates separation and recovery and is less mobile and toxic than amorphous Se^0. Insights into the interaction between selenium and sulfur bio-reduction are valuable for understanding environmental pathways and considerations regarding remediation and recovery.

* Correspondence to: P.O. Box 17, 6700 AA Wageningen, the Netherlands.
E-mail address: renata.vanderweijden@wur.nl (R.D. van der Weijden).

https://doi.org/10.1016/j.jhazmat.2022.129367
Received 15 December 2021; Received in revised form 7 June 2022; Accepted 9 June 2022
Available online 14 June 2022

1. Introduction

Anthropogenic activities, including coal combustion, mining and fertilization, release selenium oxyanions into the environment and result in selenium (Se) contamination of water and soils (Zoroufchi Benis et al., 2022). Natural sources, like the weathering of selenium-containing rocks and soils and volcanic eruptions, also contribute to selenium mobilization (Gebreeyessus and Zewge, 2019). There is a narrow range for Se concentrations when it comes to being an essential micronutrient or a toxic element with respect to Se intake (Yee, 2011; Rayman, 2012; Ullah et al., 2018). Selenite toxicity levels will lead to carcinogenic and genotoxic risks (Valdiglesias et al., 2010; Lu et al., 2017) even at low concentrations in the environment. The most common Se oxy-anions (selenate and selenite) in Se-rich water are found to be bio-accumulated in the aquatic ecosystems, resulting in reproductive and teratogenic defects for propagation and health of fish and waterfowl (Lemly, 2014; Gibson et al., 2012). Se deficiency, on the other hand, influences peoples' as well as environmental health in areas like Finland, France, and the UK (Gebreeyessus and Zewge, 2019). Recycling of Se is therefore vital for solving both the selenium contamination and scarcity.

Selenium species are often co-present with sulfur species in contaminated waters such as acid mine drainage or drainage from coals containing sulfur compounds with levels up to 43 mg Se/kg (Lenz and Lens, 2009). Run-off water from fields where fertilizer is used can also have increased Se and S levels, with up to 36 mg Se/kg (White et al., 2007). S and Se both belong to the chalcogen group and display similar chemical behavior. Both elements have multiple oxidation states, but the same biological pathway does not reach some of these states. For instance, elemental sulfur (S^0) can be formed by (partial) sulfide bio-oxidation but not by sulfate bio-reduction, whereas elemental selenium (Se^0) can be formed by selenite/selenate bio-reduction. Se-reducing bacteria play a role in the Se-cycle by selenium oxyanions bio-reduction and biomineralization using selenite/selenate as electron acceptor (Gebreeyessus and Zewge, 2019). In relation to microbial reduction reactions, sulfate can be an electron acceptor and can either inhibit or enhance selenite/selenate reducing processes (Tan et al., 2016; Wang et al., 2022). Regarding selenate, the same gene or key sulfur-assimilation enzymes can be responsible for the bio-reduction of selenate and sulfate (Ojeda et al., 2020; Huang et al., 2021) and therefore, in some studies, Se oxyanions are found to compete and inhibit the sulfate respiration or vice versa, and even inhibition of both selenate and sulfate reduction can occur at specific ratios (Zehr and Oremland, 1987; Lenz et al., 2008a; Steinberg and Oremland, 1990). In contrast, other studies found non-inhibiting or even beneficial effects on selenate removal in the presence of sulfate (Tan et al., 2018a; Hockin and Gadd, 2006; Kashiwa et al., 2000; Lortie et al., 1992; Ontiveros-Valencia et al., 2016).

Due to the (bio)chemical similarities of Se to S, the relationship of Se with S has attracted interest (Zehr and Oremland, 1987; Hockin and Gadd, 2003). Most of these studies have focused on the influence of sulfate on selenate/selenite reduction, while not much attention has been given to the influence of elemental sulfur (S^0) on the cycling of selenium and its mobility in the environment. Previous research by Hageman (Hageman et al., 2013) has shown that selenate can be anaerobically reduced to selenite by 'Eerbeek' sludge, and Hockin (Hockin and Gadd, 2003) found that selenite can be precipitated with sulfide produced by sulfate reduction to produce selenium-sulfur species. Selenium-sulfur compounds are 8-rings of variable composition (Se_nS_{8-n}) where n ranges between 2.5 and 3 (Geoffroy and Demopoulos, 2011). The formula SeS_2 is commonly used to represent these Se:S ratios (Hageman et al., 2017a). These selenium-sulfur particles were also found to be present in sulfate-rich natural waters (Piacenza et al., 2021; Vogel et al., 2018). This is in line with the research results that selenite quickly chemically reacts with sulfide to insoluble selenium-sulfur species at pH 7 (or lower) (Geoffroy and Demopoulos, 2011; Jung et al., 2016; Pettine et al., 2012).

Further bio-reduction of SeS_2 will result in crystalline black hexagonal Se^0, as demonstrated by Hageman (Hageman et al., 2017a). The hexagonal crystalline elemental selenium is thermodynamically the most stable phase. It will not be as easily oxidized as red-orange amorphous elemental selenium, which is most commonly formed extracellularly from bio-reduction of selenium oxyanions (Lenz et al., 2008a; Zambonino et al., 2021). Biologically-produced amorphous red-orange selenium cannot easily ripen to the hexagonal phase because of adsorbed organic materials like lipids, proteins, and polysaccharides (Piacenza et al., 2021). Se and S bio-cycling interactions can thus avoid this organic crystallization barrier and lead to hexagonal selenium. This will contribute to the immobilization of Se and reduction of Se toxicity in the environment by advancing bio-reduction reactions and promoting formation of a more stable phase (Hageman et al., 2017a). A list of equations for selenium and sulfur biogeochemical reduction and their possible interactions is given in Table S1.

Here, we mainly studied the effect of the addition of biologically produced S^0 on Se-oxyanion reduction using 'Emmtec' sludge, which is known to have sulfate-reducing capacity. We also made a comparison with 'Eerbeek' sludge. We postulate that when bio-S^o is co-present, bio-reduction of bio-S^o may to some extent advance the selenite reduction rate. As selenite is the intermediate in selenate reduction (Song et al., 2021), also selenate reduction may be promoted. The reaction of selenite with sulfide would result in selenium-sulfur species (SeS_2), and upon further bio-reduction, sulfide is released by the bio-reduction of sulfur present in SeS_2 and then would be available again for reacting with the remaining selenite.

2. Materials and methods

2.1. Biomass and medium

The microbial inocula used in batch experiments were two fresh granular sludges designated 'Emmtec' and 'Eerbeek'. The 'Emmtec' granules originated from a UASB reactor treating initialized process water containing only sodium sulfate and added ethanol, located in Emmen, the Netherlands (Hageman et al., 2017b), leading to very specialized microbial communities. 'Emmtec' sludge was reported to have a reducing capacity for sulfate, selenate, selenite, and SeS_2 (Hageman et al., 2017b). 'Emmtec' sludge has a volatile suspended solids (VSS) content of 0.88 $g_{VSS}/g_{dry\ weight}$, and it contains 19.9 ($\pm$ 12.3) mg S_{total} per gram dry weight (D'Abzac et al., 2010).

In comparison, 'Eerbeek', which is mainly methanogenic, originated from a full-scale UASB reactor treating highly complex wastewater from a paper factory in 'Eerbeek', the Netherlands. Besides methane production, sulfate reduction, selenate reduction, and selenite reduction were also reported for this biomass (Lenz et al., 2008a; Hageman et al., 2013; Astratinei et al., 2006). 'Eerbeek' sludge has a VSS content of 0.74 $g_{VSS}/g_{dry\ weight}$. The 'Eerbeek' sludge used in these experiments contains 16.1 ($\pm$ 3.1) mg S_{total} per gram dry weight (D'Abzac et al., 2010).

The elemental sulfur added to solutions was biologically generated sulfur from a Thiopaq sulfide oxidizing bioreactor located at a bio-waste treatment plant in Germany. The bio-sulfur (bio-S^0) was washed with MilliQ water three times and dried before use in experiments. This process was repeated twice. The ground bio-S^0 particles were sieved to a particle size $\leq$ 200 μm. More detailed information on the treatment and characterization of the bio-S^0 is given in Hidalgo-Ulloa et al., 2020.

The medium used in batch experiments was adapted from Stams (1992), excluding sodium selenite, sodium hydrogen carbonate, and sodium sulfide (Hageman et al., 2013). The medium consisted of (g/L): $Na_2HPO_4{\cdot}2H_2O$ (0.53), KH_2PO_4 (0.41), NH_4Cl (0.3), $CaCl_2{\cdot}2H_2O$ (0.11), $MgCl_2{\cdot}6H_2O$ (0.10), and acid- and base trace elements and vitamin solution (Stams et al., 1992). The pH of the medium was adjusted to pH 7 by using hydrogen chloride or sodium hydroxide. The reagents were of analytical grade unless stated otherwise.

2.2. Batch experiments

Batch experiments were carried out in duplicate in 125 mL glass bottles with 25 mL medium containing ~2 mmol L^{-1} selenite or ~2 mmol L^{-1} selenate and for both using 1.25 and 2.5 mmol L^{-1} lactic acid as an electron donor. The culture bottles were closed with a butyl rubber stopper, and an aluminum crimp seal. The headspace was degassed to 0.5 atm and then gassed to 1.5 atm with 100% N_2. This step was repeated five times with a final overpressure of 0.5 atm of N_2. The bottles were incubated in a shaker (120 rpm) at 30 °C. Control experiments without sludge were carried out under the same conditions.

Control experiments with inactive biomass were also carried out to investigate the potential chemical reactions between selenite and reductants that might be initially present in the sludge. The microbial activity was inhibited by adding 0.02% NaN_3 to batch bottles, which contained 1.2 g_{VSS} L^{-1} 'Emmtec'or 'Eerbeek' sludge with ~2 mmol L^{-1} selenite or selenate using 1.25 mmol L^{-1} lactic acid as the electron donor. The NaN_3 was refreshed every 3 days. Other conditions (initial pH, temperature, gas composition in headspace, incubator settings) were the same as in the selenite/selenate bio-reduction experiments.

Besides, to investigate the bio-reduction activity by 'Emmtec'or 'Eerbeek' sludge on removing sulfur species (1 mmol L^{-1} bio-S^0 or sulfate), another series of control experiments were done by excluding selenite and selenate from the medium. The other conditions (medium composition, pH, temperature, sludge type and concentrations, incubator settings, etc.) were kept the same as mentioned above.

Different amounts of bio-S^0 (0, 1, 2, 4 mmol L^{-1}) or 1 mmol L^{-1} sodium sulfate were added to batch bottles to investigate the interaction between Se and S.

2.3. Analysis and calculation

Liquid samples were taken with a syringe and filtered over a 0.20 μm filter. Dissolved selenate and selenite concentrations were analyzed by ion chromatography (Dionex ICS 2100, Thermo Fisher Scientific, Waltham, MA, USA). The sulfide concentration was measured using a Hach Lange test LCK-635 and a Hach Lange Xion 500 spectrophotometer. The total selenium was analyzed at a wavelength of 196 nm by inductively coupled plasma optical emission spectrometry (ICP-OES) equipped with an MPX megapixel detector (VISTA-MPX CCD Simultaneous, VARIAN co.). The solid samples were washed as described by Hageman (Hageman et al., 2017b) and characterized by light microscopy with a Nikon Eclipse E400 (1000x magnification, Nikon, Tokyo, Japan) and X-ray diffraction (XRD) on a Bruker D8 advanced diffractometer equipped with a Vantec position sensitive detector and with a Co Kα radiation (λ = 0.179 nm) over a range of 10–70° with a step size of 0.02and a step time of 0.1 s. DIFFRAC.EVA (version 5.0, Bruker AXS, Karlsruhe, Germany).

The experiments were evaluated for selenite and selenate removal efficiency ($R_{selenite}$, $R_{selenate}$, respectively), as calculated with the following equations:

$$R_{selenite} = (1 - \frac{C_{selenite}}{C^0_{selenite}}) \times 100\% \quad (9)$$

$$R_{selenate} = (1 - \frac{C_{selenate}}{C^0_{selenate}}) \times 100\% \quad (10)$$

Where $C^0_{selenite}$, $C^0_{selenate}$ is the initial concentration of selenite/selenate, $C_{selenite}$ and $C_{selenate}$ is the concentration of selenite/selenate left in the liquid phase.

3. Results and discussion

The potential reaction routes investigated here for Se-oxyanion reduction in the presence of sulfur species are shown in Fig. 1.

3.1. Effects of elemental sulfur (bio-S^0) on the removal of selenite with 'Emmtec'

Using about a 1:1 molar ratio of selenite and bio-S^0, and assuming bio-cycling of sulfur resulted in precipitation of SeS_2 (Fig. 1 green part), 'Emmtec' sludge had a higher removal rate for selenite with bio-S^0 than without bio-S^0 addition (Fig. 2). In the first three days, no significant difference in the residual selenite concentration with or without bio-S^0 was found (1.70, 1.74 mmol L^{-1} on day 3 in experiments with 1.92 mmol L^{-1} selenite, respectively). Microorganisms first need to start to bio-reduce solid bio-S^0 into sulfide. On day 7, the difference between experiments with and without bio-S^0 became clearer and even more so on day 20; 0.45 versus ~0, and 0.55 versus 0.16 mmol L^{-1} of selenite remained from starting concentrations of 1.73 and 1.92 mmol L^{-1}, respectively. Control experiments without sludge or with inactivated sludge did not show any selenite concentration change in 20 days, affirming that selenite does not adsorb to or react with bio-S^0 during this experiment time, and no sulfide is bio-generated.

There is a remarkable difference in the type of solids formed. After 20 days (Fig. 3A), XRD analysis showed that addition of bio-S^0 resulted in more hexagonal Se^0, although amorphous red selenium is still present. In the study of Hageman (Hageman et al., 2017a), it was shown that further reduction of SeS_2 leads to black hexagonal Se^0 nanoparticles. The green line in Fig. 3A represents seven hexagonal Se^0 peaks in the range of 20–60 °2θ from the particles formed in the experiments with bio-S^0, sampled on day 20. No hexagonal Se^0 peaks matched the black line of the particles formed in the experiments without bio-S^0, sampled on day 20. By using DIFFRAC.EVA, it could be estimated that the crystallinity on day 20 had increased from 6.1% of a global area of 316.24 in the experiment without bio-S^0 to 13.0% of a global area of 300.76 with sulfur addition. These results show that the addition of bio-S^0 promotes the formation of black crystalline Se^0.

The different solids' morphology was also indicated by the color change with time. At the start of each batch experiment, the medium was colorless and transparent, with only the black granular biomass visible as solids. Without added bio-S^0, red attachments were found on the surface of the granules from day 3 onwards. Red suspensions made the liquid appear pinkish by day 3. Then, the liquid's color became lighter while the red attachment became darker red than before (Fig. 3B-1). The color change in this experiment is in line with findings in the selenite bio-reduction study by Gonzalez-Gil (Gonzalez-Gil et al., 2016).

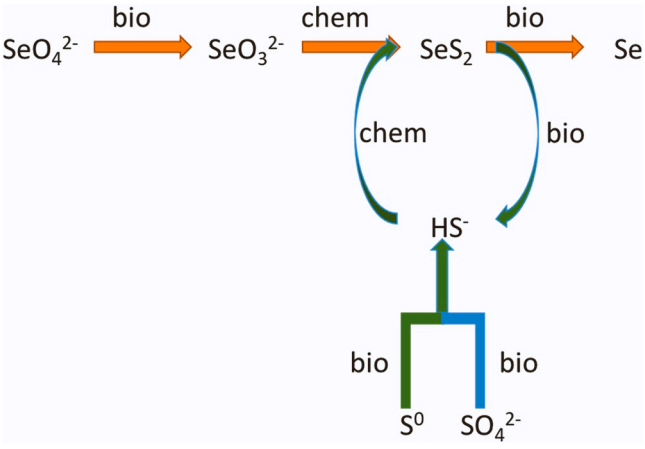

Fig. 1. Potential reaction routes to reduce the toxic Se oxy-anion mobility in the environment by reducing soluble selenate or selenite to Se^0 with S bio-cycling. When selenite is present or produced as the intermediate from selenate bio-reduction, it could chemically react with the produced sulfide from the bio-reduction of sulfur species to form SeS_2. SeS_2 would then be bio-reduced to elemental selenium and sulfide, and the latter becomes available to react with selenite again.

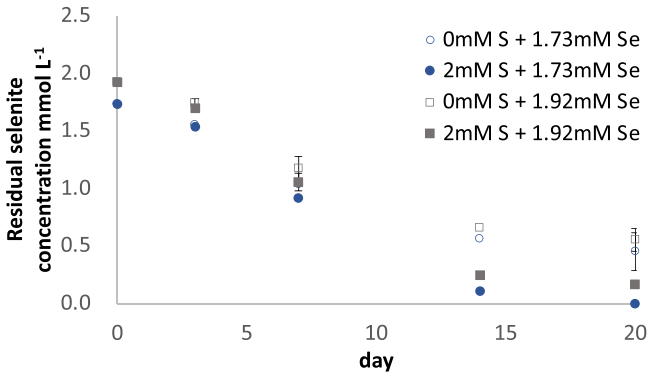

Fig. 2. Bio-sulfur (bio-S^0) increases the selenite removal rate using 'Emmtec' sludge. Conditions: 1.2 g_{VSS} L^{-1} 'Emmtec' sludge, 30 °C, pH 7, initial selenite concentration: 1.73 or 1.92 mmol L^{-1}, using 1.25 mmol L^{-1} lactic acid as electron donor: 1.92 mmol L^{-1} selenite, no sulfur (□); 1.92 mmol L^{-1} selenite, 2 mmol L^{-1} bio-S^0(■); 1.73 mmol L^{-1} selenite, no bio-S^0 (○); 1.73 mmol L^{-1} selenite, 2 mmol L^{-1} bio-S^0(●).

Microscopy (Fig. 3B-3) showed that the red solids were spherical particles, either attached to the 'Emmtec' granules or suspended in solution while being attached to suspended bacteria. However, with bio-S^0 addition, the liquid's color was orange-red, and the orange-red attachment on the granules became black-red by day 20 (Fig. 3B-4,5). Both spherical and acicular solids were found in this experiment on day 20. Specifically, the black particles collected on the bottom of the batch assay were clusters of acicular particles (Fig. 3B-6), indicating the production of hexagonal crystalline Se^0.

Regarding the Se recovery potential, the formation of the hexagonal Se^0 is more favorable compared to the amorphous Se^0 due to the former's properties of higher density, less attachment to biomass, the bigger (crystal) size (≥10 μm as shown in Fig. 3B-6), leading to a faster settlement from the treated water and easier separation from the biomass (Hageman et al., 2017b; Alivisatos, 2000; Minaev et al., 2005). The formation of hexagonal Se^0 also has a lower potential environmental risk because of its thermodynamic stability and lower oxidation potential compared to amorphous Se^0. Also, amorphous Se^0 was reported to remain stable as colloidal suspensions in the aquatic system for weeks and could be remobilized to Se-oxyanions in the oxygenated zones of water bodies (Tan et al., 2016).

3.2. Sulfur cycling: effects of different elemental sulfur concentrations on selenite removal

The sulfide bio-production from bio-S^0 was also investigated (Fig. 4A). No sulfide was detected in the control solutions on all sampling days. Any sulfide produced by sulfur already present in the original 'Emmtec' in the batch without bio-S^0 was too small to be considered to play a role in selenite removal. More sulfide was produced with higher amounts of bio-S^0. What can be assumed is that the addition of bio-S^0 produced sulfide (tested in experiments without selenite) and promoted selenite removal efficiency. However, the aqueous sulfide measured was less than the amount that could be produced by a complete bio-S^0 reduction (based on equation 2). At the experimental pH of 7, nearly half of the produced sulfide is present as H_2S and resides in the headspace, and the bio-S^0 bio-reduction may not have been completed in 20 days.

To better understand whether bio-S^0 plays a role in selenite conversion to crystalline elemental selenium, the effects of various amounts of bio-S^0 during selenite removal were studied. Surprisingly, an increase in the amount of bio-S^0 did not increase the selenite removal rate (Fig. 4B). On day 7, an average of 0.83, 0.92, and 0.79 mmol L^{-1} selenite was left in the batch bottle with 1, 2, and 4 mmol L^{-1} bio-S^0, respectively. On day 20, a negligible concentration of selenite was left for all bio-S^0 concentrations ($1.6 \times 10^{-4} \pm 3.7 \times 10^{-5}$, $1.2 \times 10^{-4} \pm 7.8 \times 10^{-6}$, and $5.8 \times 10^{-3} \pm 8.0 \times 10^{-3}$ mmol Se L^{-1} respectively). The sulfide present in the solution was determined on days 3, 7, 14, and 20. Aqueous sulfide could only be detected on day 20 when all selenite had been reduced. The concentrations measured on day 20 were 0.33, 0.37, and 0.55 mmol L^{-1} in bottles with 1, 2, and 4 mmol L^{-1} bio-S^0, respectively. This indicates that bio-S^0 is bio-reduced to sulfide and followed by a reaction with selenite to produce (amorphous) SeS_2 alongside the biological conversion of selenite to red amorphous elemental selenium, after which S in SeS_2 is reduced to sulfide.

Furthermore, with the reported chemical reaction kinetics between selenite and sulfide (Jung et al., 2016), the estimated S^0 bio-reduction rate (according to Fig. 4A) was not high enough to remove all selenite via the chemical precipitation of SeS_2 (according to the varied S: Se ratio (1.7–2.3) reported in previous research to eliminate selenite by sulfide (Geoffroy and Demopoulos, 2011)); also direct biomineralization was on-going. Even when assuming all bio-S^0 can be reduced to sulfide, only the maximum sulfide production (4 mmol L^{-1}) might be sufficient for complete selenite removal as SeS_2. However, the sulfide that is introduced can cycle according to the sulfur bio-cycling pathway (Fig. 1, green part), where Se^0 particles can be formed when sulfur (in SeS_2) is reduced and becomes available again as sulfide. So we speculated that sulfur is re-introduced and can react again with selenite, and so less bio-S^0 is needed to reduce selenite because of bio-S^0 cycling (Fig. 1). According to thermodynamic data (Equation 4, Table S1), bio-reduction of SeS_2 may even be slightly more favorable than bio-S^0 bio-reduction.

Evidence for SeS_2 was found twice by XRD; analysis of the solids in the experiment with bio-S^0 on day 3 did have a signal matching with the SeS_2 crystal pattern, but there was not enough sample mass to produce a more convincing result. Furthermore, SeS_2 may also be amorphous and thus not be detected by XRD. Most of the time, the XRD analysis for samples to which bio-S^0 was added showed crystalline Se^0, which means that the SeS_2 had been further reduced. The produced solids were also inspected for composition by digesting sludge granules with precipitates attached with ICP-OES. This confirmed the presence of selenium for both experiments, with and without bio-S^0.

3.3. Effects of sulfate on bioconversion selenite to selenium by 'Emmtec' sludge

As it is difficult to follow the solid bio-S^0 concentration change without sacrificing the entire solids content (organics as well) for analysis, we included batch experiments with sulfate for 'Emmtec', as soluble sulfur species can be followed in solution to better understand the biochemical interaction between selenite and co-existing sulfur species. Fig. 5A shows that sulfate, after bio-reduction to sulfide, like bio-S^0, can also accelerate the selenite bio-reduction rate. However, the average selenite removal rate with one mmol L^{-1} sulfate was much higher than with one mmol L^{-1} bio-S^0 (22 and 5 mg Se g_{VSS}^{-1} L^{-1} in 3 days, respectively, with sulfate and bio-S^0, and 13 and 8 mg Se g_{VSS}^{-1} L^{-1} in 7 days, respectively, with sulfate and bio-S^0). One needs to keep in mind that 'Emmtec' sludge came from a plant where it reduced sulfate and not bio-S^0. Moreover, solid bio-S^0 is not as homogeneously mixed and bioavailable, so it may be more challenging to reduce bio-S^0 due to physical limitations, and at a pH of 7, significant solubilization of sulfur by the formation of polysulfides is not expected (Chen and Gupta, 1973; Millero, 1986).

Hockin (Hockin and Gadd, 2003) mentioned that 200 μmol L^{-1} selenite is the subinhibitory concentration for sulfate-reducing bacteria, and found that selenite and sulfate reduction gave rise to Se and S formation in a biofilm without mentioning the in-between product of SeS_2. In this experiment, the sulfate concentration dropped faster in the bottle with selenite than without selenite (used as a control) (Fig. 5B). Therefore, an interaction of the two bio-reduction processes is assumed, such as SeS_2 formation, that positively affected both rates. In another study, it was found that sulfate did not inhibit selenite reduction, as selenite is reduced by the sulfite reductase-mediated pathway and that

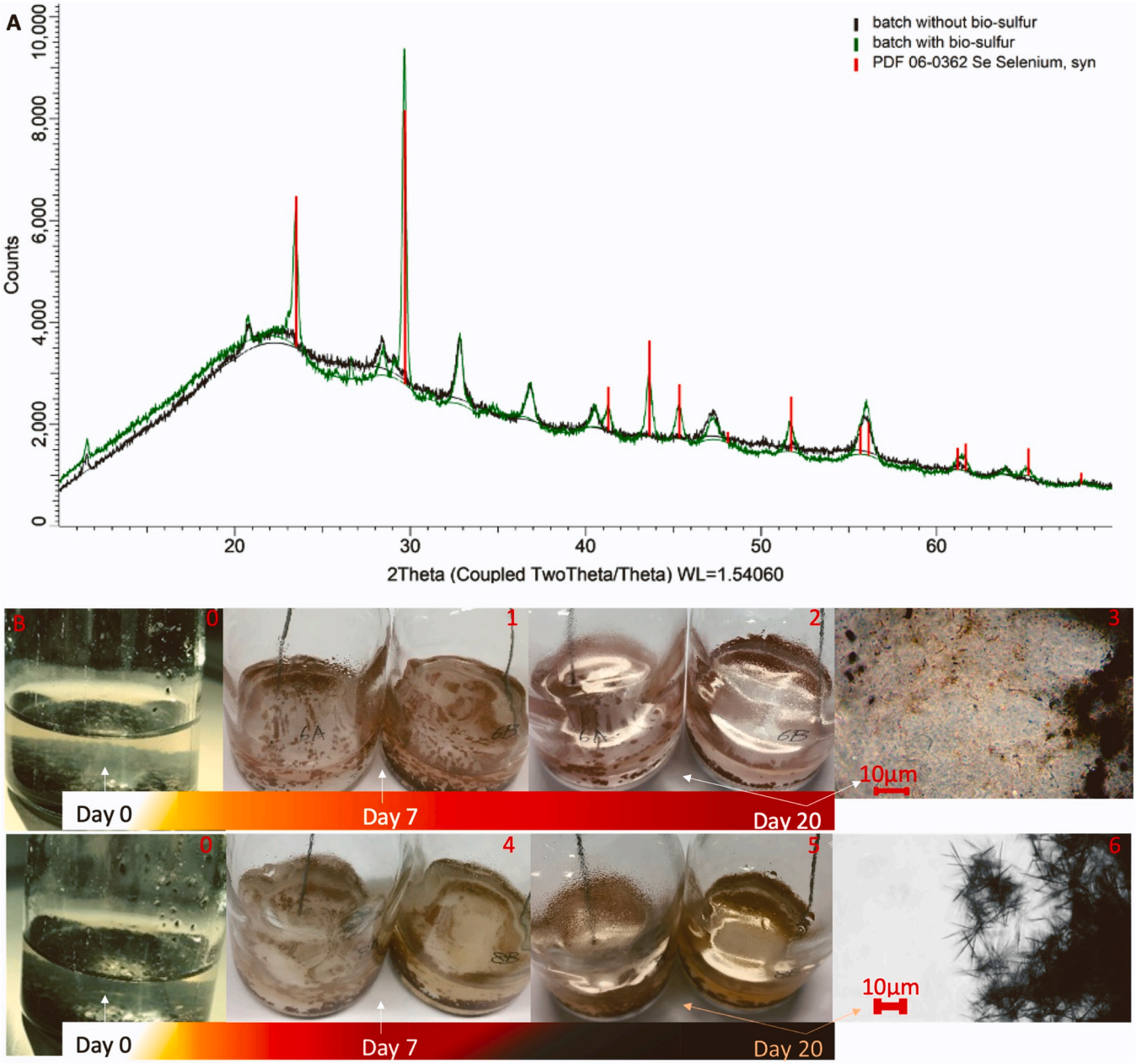

Fig. 3. A XRD results on day 20 confirmed that crystalline Se^0 solids are present in the experiments with bio-sulfur (bio-S^0) addition but not in experiments without bio-S^0. Legend: Black line- particles formed in the experiments without bio-S^0 addition, sampled on day 20; Green line- precipitate formed in the experiments with 2 mmolL^{-1} bio-S^0, sampled on day 20; Red line- hexagonal Se^0 in database. Fig. 3**B** The color and solid structure change in the experiment with and without bio-S^0 on day 7 and 20. (0) Batch assay without bio-S^0 on day 0; (1) Batch assay without bio-S^0 on day 7; (2) Batch assay without bio-S^0 on day 20; (3) Microscope observation of solids in batch without bio-S^0 on day 20; (4) Batch assay with bio-S^0 on day 7; (5) Batch assay with bio-S^0 on day 20; (6) Microscope picture of the acicular cluster in batch with bio-S^0 on day 20. Conditions: 1.2 g_{VSS} L^{-1} 'Emmtec' sludge, 30 °C, pH 7, initial selenite concentration: 1.92 mmol L^{-1}, using 1.25 mmol L^{-1} lactic acid, 0 or 2 mmol L^{-1} bio-S^0.

treatment with selenite upregulated the sulfate assimilation pathway enzymes (Huang et al., 2021).

The sulfide production in control experiments by one mmol L^{-1} of sulfate (Fig. 5B) was higher than by one mmol L^{-1} of bio-S^0 measured on day 3, 7, and 14, respectively, but was similar on day 20 (0.38 mmol L^{-1} by sulfate and 0.34 mmol L^{-1} with bio-S^0). The sulfide production by one mmol L^{-1} of sulfate was even higher than the production by 4 mmol L^{-1} of bio-S^0 on day 3 and similar on day 7 (Fig. 5B), which explains why more selenite was removed by 1 mmol L^{-1} sulfate than bio-S^0 in the first 7 days. It also shows that chemical precipitation is apparently faster than direct bio-reduction of selenite.

Similar to experiments with bio-S^o, with selenite present, sulfide was only found after selenite was removed entirely after day 14 and reached a similar final sulfide level on day 20 as in control experiments without selenite. The sulfide production from day 14 to day 20 cannot be explained by direct sulfate bio-reduction to sulfide, from which it can be concluded that there should be sulfide production by bio-reduction of SeS_2. This result suggests that sulfide produced in the experiments by sulfate reduction was used immediately to reduce selenite to SeS_2 and was released again (see blue and green-blue arrow, Fig. 1) to the system by bio-reduction of SeS_2. As shown in Fig. 5B, 0.44 mmol L^{-1} sulfide was produced from day 14–21, while during this period, only 0.05 mmol L^{-1} sulfate was reduced, indicating an average production rate of 0.067 mmol L^{-1} day^{-1} (by bio-reduction of SeS_2). This rate is higher than

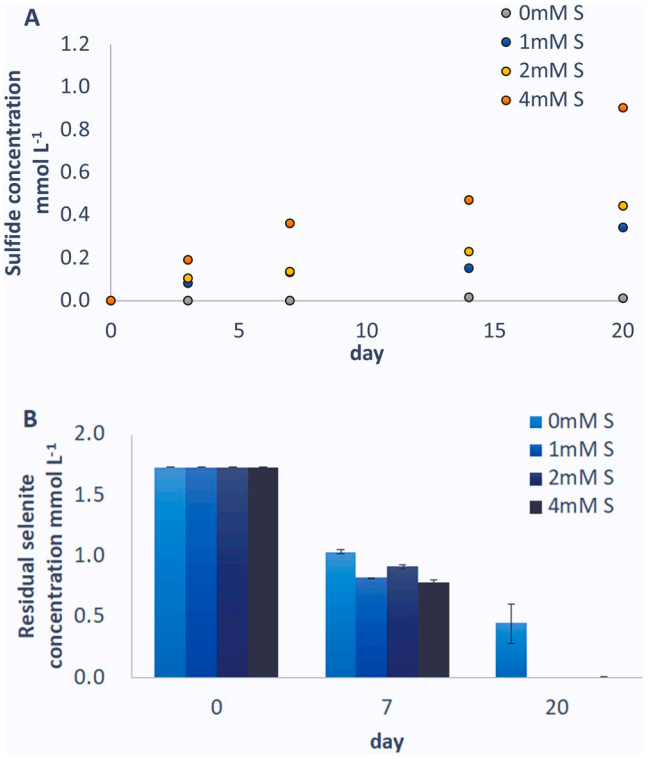

Fig. 4. A Sulfide produced from bio-S^o in experiments without selenite. Conditions: 1.2$g_{VSS}L^{-1}$ 'Emmtec' sludge, 30 °C, pH 7, initial selenite concentration: 0 mmol L^{-1}, using 1.25 mmol L^{-1} lactic acid as electron donor. Legend: no sulfur addition (●); with initial 1 mmol L^{-1} bio-S^0 (●); with initial 2 mmol L^{-1} bio-S^0 (●); with initial 4 mmol L^{-1} bio-S^0 (●). **Fig 4B** The selenite removal rate increases in the presence of bio-sulfur (bio-S^0), but a further increase in amounts of bio-S^0 did not increase the rate using 'Emmtec'. Conditions: 1.2$g_{VSS}L^{-1}$ 'Emmtec' sludge, 30 °C, pH 7, initial selenite concentration: 1.73 mmol L^{-1}, using 1.25 mM lactic acid as electron donor. Legend: no sulfur addition (■); with initial 1 mmol L^{-1} bio-S^0 (■); with initial 2 mmol L^{-1} bio S^0 (■); with initial 4 mmol L^{-1} bio S^0 (■).

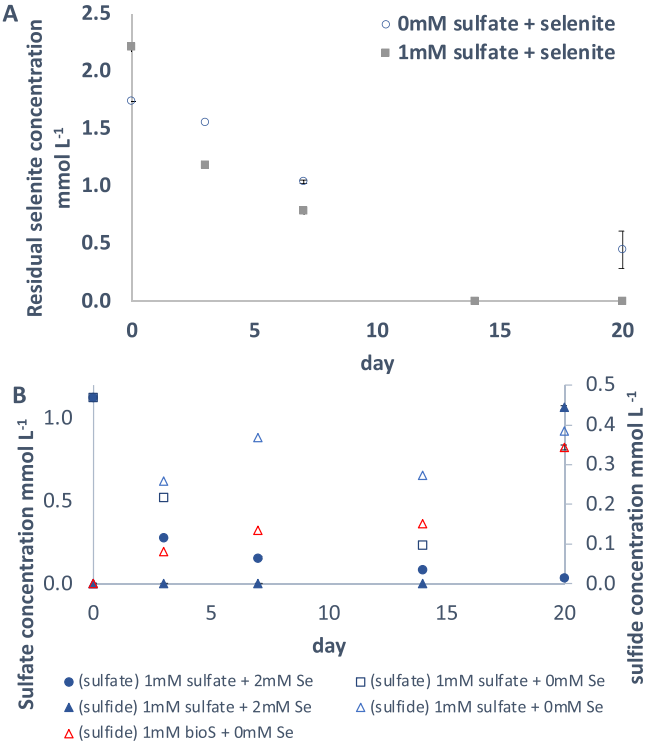

Fig. 5. A Sulfate addition increases the selenite removal rate for 'Emmtec' sludge. Conditions: 1.2gVSS/L 'Emmtec' sludge, 30 °C, pH 7, initial selenite concentration: 1.73 or 2.2 mmol L^{-1}, using 1.25 mM lactic acid as electron donor, 0 or 1.12 mmol L^{-1} sulfate. Legend: 1 mmol L^{-1} sulfate (■); no sulfate (○). Fig. 5B. Sulfate concentration and sulfide concentration change with and without selenite present. Conditions: 1.2$g_{VSS}L^{-1}$ 'Emmtec' sludge, 30 °C, pH 7, initial selenite concentration: 0 or 2.2 mmol L^{-1}, using 1.25 mM lactic acid as the electron donor, 0 or 1.12 mmol L^{-1} sulfate, and 0 or 1 mmol L^{-1} bio-S^0. Legend: sulfate concentration in the experiment with 1 mmol L^{-1} sulfate and 2 mmol L^{-1} selenite (●); sulfate concentration in the experiment with 1 mmol L^{-1} sulfate and 0 mmol L^{-1} selenite (□); sulfide concentration in batch with 1 mmol L^{-1} sulfate and 2 mmol L^{-1} selenite(▲); sulfide concentration in batch with 1 mmol L^{-1} sulfate and 0 mmol L^{-1} selenite (△); sulfide concentration in batch with 1 mmol L^{-1} bio-S^0 and 0 mmol L^{-1} selenite (△).

the highest rate of sulfide production by 1 or 2 mmol L^{-1} bio-S^0 (Fig. 4A) and may explain the minor differences in residual selenite concentrations using different amounts of bio-S^0.

The higher sulfide production rate was also reflected in the color development: with SO_4^{2-} the color became darker (blackish) already after day 7. Again the black product indicated crystallization to hexagonal Se^0.

3.4. Effect of an increase in electron donor concentration on the removal rate of selenite

We also studied the effect of the electron donor concentration using 1.2 g_{VSS} L^{-1} 'Emmtec' sludge, as this may affect rates of bio-S^o/bio-sulfate reduction and/or selenite bio-reduction differently. When doubling the electron donor concentration, the selenite removal rate increased in experiments with and without sulfur compounds (Fig. 6 A). The sulfate reduction rate also increased with an increase in the electron donor concentration (Fig. 6B). However, the increase in the selenite removal rate using an increased electron donor concentration with one mmol L^{-1} sulfate is more significant than the increase in the sulfate removal rate, which could mean that bio-reduction of selenite is relatively more promoted or that SeS_2 bio-reduction is more significantly promoted.

3.5. Effects of the biomass concentration on the interaction between selenium and bio-sulfur by 'Emmtec' sludge

Experiments with 2.8 g_{VSS} L^{-1} 'Emmtec' instead of 1.2 g_{VSS} L^{-1} 'Emmtec' (with and without bio-S^0) were carried out to determine the effect of increasing the biomass (VSS) concentration. The increased concentration of 'Emmtec' sludge increased the selenite removal rate and accelerated the recrystallization to black selenium. The selenite was removed so fast by 2.8 g_{VSS} L^{-1} 'Emmtec' that the removal efficiency amounted to 99.9% within 3 days, irrespective of the addition of bio-sulfur. The color of suspensions changed from orange-red to black on day 7–20 (Fig. S1).

Black hexagonal crystals can be the result of the aggregation of amorphous elemental selenium and subsequent crystallization (Song et al., 2021), which nowadays has been recognized as a non-classical crystallization route (De Yoreo et al., 2015), or via bio-reduction of sulfur from SeS_2 (Equation 4, Table S1). Increasing the biomass concentration would accelerate both routes. As shown in Fig. 2, compared to the biochemical reaction with sulfide, bio-reduction of selenite is the more dominant process for removing selenite. Besides, the selenite reduction was almost completed on day 3 in this experiment, leaving a longer time for aggregation and (re)crystallization until day 20.

3.6. Effects of bio-S^0 on selenate removal by 'Emmtec'

Should selenate be present, then it was hypothesized that since selenite is the intermediate reduced species, perhaps the addition of bio-S^0 could positively affect the selenate reduction rate (Fig. 1).

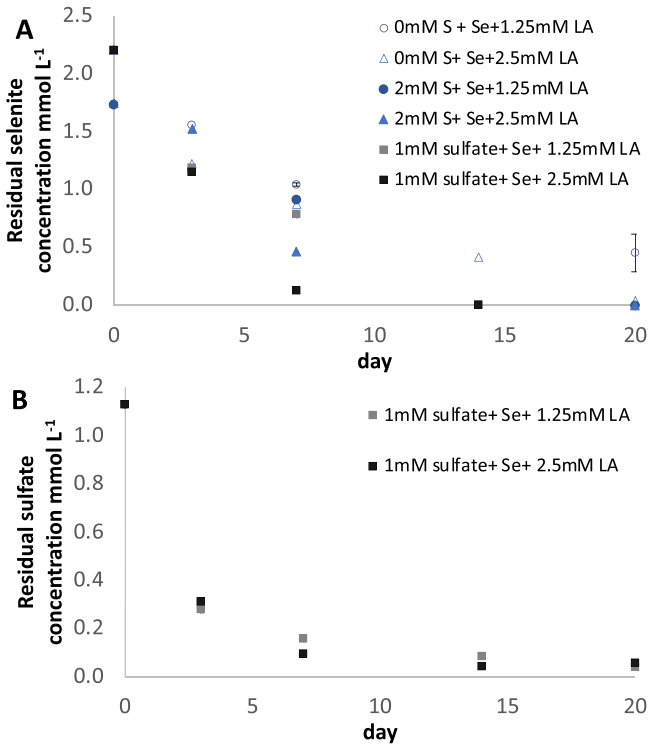

Fig. 6A. An increase in the electron donor concentration accelerates the selenite removal. Conditions: 1.2 g_{VSS} L^{-1} 'Emmtec' sludge, 30 °C, pH 7, no sulfur with 1.25 mmol L^{-1} lactic acid and 1.73 mmol L^{-1} initial selenite (○), 2 mmol L^{-1} bio-S^0 with 1.25 mmol L^{-1} lactic acid and 1.73 mmol L^{-1} initial selenite (●), no sulfur with 2.5 mmol L^{-1} lactic acid and 1.73 mmol L^{-1} initial selenite (△), 2 mmol L^{-1} bio-S^0 with 2.5 mmol L^{-1} lactic acid and 2.2 mmol L^{-1} initial selenite (○),1 mmol L^{-1} sulfate with 1.25 mmol L^{-1} lactic acid and 2.2 mmol L^{-1} initial selenite (●), 1 mmol L^{-1} sulfate with 2.5 mmol L^{-1} lactic acid and 2.2 mmol L^{-1} initial selenite (▲); **Fig. 6B** An increase in the electron donor concentration accelerates the sulfate removal. Conditions: 1.2 g_{VSS} L^{-1} 'Emmtec' sludge, 30 °C, pH 7, initial selenite concentration: 2.2 mmol L^{-1}, 1 mmol L^{-1} sulfate with 1.25 mmol L^{-1} lactic acid (■), 1 mmol L^{-1} sulfate with 2.5 mmol L^{-1} lactic acid (▲).

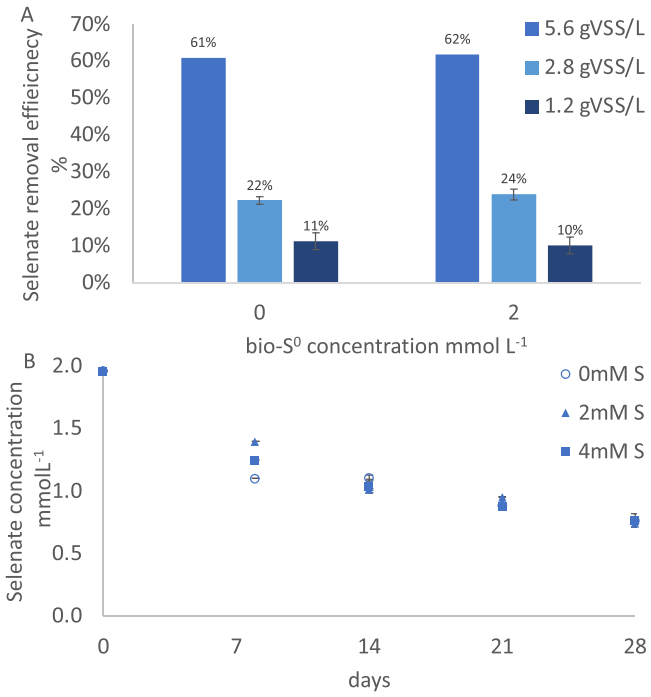

Fig. 7. A The effects of 2 mmol L^{-1} bio-S^0 on selenate removal efficiency by different amounts of 'Emmtec' sludge by day 21. Legend: 5.6 g_{VSS} L^{-1} 'Emmtec' with 1.25 mmol L^{-1} LA (■); 2.8 g_{VSS} L^{-1} 'Emmtec' with 1.25 mmol L^{-1} LA (■);1.2 g_{VSS} L^{-1} 'Emmtec' with 1.25 mmol L^{-1} LA (■). Conditions: 30 °C, pH 7, initial selenate concentration: 1.96 mmol L^{-1}, using 1.25 mmol L^{-1} lactic acid as the electron donor. Fig. 7**B** The residual selenate concentration versus time by 5.6 g_{VSS} L^{-1} 'Emmtec' with different concentrations of bio-S^0; legend: no sulfur addition (○); with initial 2 mmol L^{-1} bio-S^0 (▲); with initial 4 mmol L^{-1} bio-S^0 (▲). Conditions: 30 °C, pH 7, initial selenate concentration: 0 or 1.96 mmol L^{-1}, using 1.25 mmol L^{-1} lactic acid as the electron donor.

In the absence of bio-S^0, 11 ± 2% selenate was removed by 1.2 g_{VSS} L^{-1} of 'Emmtec' sludge by day 21, as shown in Fig. 7. The addition of 2 mmol L^{-1} bio-S^0 did not show much difference in the removal efficiency (10 ± 2% by day 20) compared to assays without bio-S^0. An attempt to increase the selenate removal performance by increasing the biomass concentration was made. Increasing the biomass concentration up to 5.6 g_{VSS} L^{-1} notably increased the removal efficiency of 'Emmtec' sludge to 61%. The addition of 2 mmol L^{-1} bio-S^0 did not significantly contribute to the selenate removal efficiency (62%). Regardless of any possible bio-S^0 effects, the higher selenate reduction rate by increasing the amount of sludge can be explained by the increased biomass concentration (for faster selenate reduction) and the increased endogenous substrate initially present in the sludge; the latter was reported to illustrate the selenate removal in experiments using 'Eerbeek' sludge without an external electron donor (Astratinei et al., 2006).

However, in the first seven days, for the various biomass concentrations (Fig. 7B, only showed the results with 5.6 g_{VSS} L^{-1} 'Emmtec'), when most selenate is reduced (~44% in assays without bio-S^0), an adverse effect of bio-S^0 was seen. Comparing the positive effects of sulfur in selenite assays and the fact that 'Emmtec' originated from a sulfate-reducing reactor, the toxicity of produced sulfide on 'Emmtec' sludge that inhibited the selenate removal activities may be excluded. The high sulfide tolerance of bacteria, which reduced selenate in the sulfate-reducing bioreactor, was reported before (Lenz et al., 2008a). One explanation is that as the same enzymes can be responsible for both selenate and sulfate reduction (Tan et al., 2018b), the same can be true for elemental sulfur reduction which could result in competition effects. Furthermore, the selenite bio-reduction intermediate (Hageman et al., 2013; Song et al., 2021; Astratinei et al., 2006), that was determined in solutions in studies when the reduction potential increased, may not have been long-lived or released in solution. Instead, it was subsequently immediately bio-reduced to elemental selenium close to or on the cell wall. We had noticed that initially the produced red amorphous selenium stuck to the granule surface. If this is the case, there is hardly any scavenging of selenite by sulfide in solution, and bio-S^o reduction would just compete with selenate reduction. Furthermore, selenite was not found in all experiments when sampling on day 3, 7, 14, 21, and 28.

3.7. *Effects of bio-S^0 on selenite and selenate removal by 'Eerbeek' sludge*

As 'Eerbeek' sludge has been previously investigated for biological selenate reduction also in the presence of sulfate (Lenz et al., 2008a; Hageman et al., 2013; Song et al., 2021; Astratinei et al., 2006), assays with this sludge were also carried out to compare the selenite/selenate removal capacity using bio-S^o with the same VSS concentration as for 'Emmtec' (Tables ^{1}A–^{1}B).

From a control experiment with 1.2 g_{VSS} L^{-1} sludge and 1 mmol L^{-1} bio-S^0 and measuring sulfide production, it was apparent that 'Eerbeek' sludge has a lower bio-S^0 reducing capacity and rate than 'Emmtec' sludge. Also for 1 mmol L^{-1} sulfate, the sulfide production rate was lower for 'Eerbeek' than for 'Emmtec'. So we expected a lower effect of adding bio-S^0 on both selenite and selenate reduction. The addition of bio-S^o still had a small positive effect on the selenite removal rate, which without bio-S^o was already higher than for 'Emmtec' (Table 1A). As the progress of bio-reduction of selenite without bio-S^0 was already 75%

after 7 days (compare to 32% for 'Emmtec') and sulfide formation is slow, the positive effect of bio-S^0 is less visible. Yet, we still see a positive effect of a 14% increase with 4 mmol L^{-1} bio-S^0 and conclude that this is related to selenium sulfide formation and its further bio-reduction. Therefore, also more hexagonal Se is formed with the addition of bio-S^0 though less than for 'Emmtec'.

Regarding the differences in selenate removal performance in response to bio-S^0 addition for the two sludges, it was found that the 5.6 g_{VSS} L^{-1} 'Emmtec' sludge showed a higher selenate removal rate than the same biomass concentration of 'Eerbeek', irrespective of the amount of bio-S^0. Moreover, 'Emmtec' also performed better for 1.2 and 2.8 gvss L^{-1} (Table 1B). 'Emmtec' is dominantly a sulfate-reducer, and as the same enzymes can reduce both sulfate and selenate (Tan, 2018), the higher selenate bio-reduction rate for 'Emmtec' can be understood accordingly. For 'Eerbeek', with the addition of bio-S^0, a very slight acceleration and increase in the selenate removal was found over the entire experimental runtime. For 'Emmtec', as mentioned in the previous section, also minimal effects were seen. Co-presence of bio-S^0 therefore seems to be a more prominent factor for hexagonal selenium formation when selenite is present in solution or when it is produced as an intermediate product of selenate reduction and is released in solution, as seen in Song et al., 2021. The different effects of bio-S^0 for these two types of sludge must be related to the complex interaction between bio-S^0/selenite/selenate/SeS_2 reduction capacity and kinetics.

3.8. The morphologies of the final Se-products

The selenite abiotic reduction to elemental selenium has been discussed in other research (Hockin and Gadd, 2003; Geoffroy and Demopoulos, 2011; Pettine et al., 2012), and the chemical interaction between sulfide and selenite is more complex than the production of selenium-sulfur SeS_x, here simplified to SeS_2 (Kharma et al., 2019), making it difficult to track the interaction between selenite and bio-S^0.

As a result of the interaction, the morphologies of the final Se-products (solids collected at the end of each experiment: day 20, Fig. 8) had apparent differences for different conditions. We can hardly find any acicular Se^0 crystals produced from the selenite reduction by 'Emmtec' sludge without bio-S^0. Mostly spherical amorphous Se^0 particles (confirmed by EDS) are present as single particles or attached to the granules, which is in line with the reported selenium spheres formed in other bio-processes (Gonzalez-Gil et al., 2016). With bio-S^0 addition, acicular Se^0 crystals were easily detected. This finding is in line with the XRD results (Fig. 3A), where we found a crystalline signal only in the experiments with bio-S^0 addition.

For 'Eerbeek' assays, Se^0 crystals were found in the final product for both conditions with and without bio-S^0 addition. The latter showed large hexagonal Se^0 crystals of ~20 μm (in length) (see the circle in Fig. 8) and large numbers of small amorphous Se^0 particles growing in the surroundings or even on the crystals faces (as can be seen in the crystalline C-axis direction for the hexagonal system). The hexagonal Se^0 could be recrystallized by the aggregation of amorphous Se^0, due to the fact that the amorphous structure is thermodynamically unstable so that it would slowly recrystallize by aging (Song et al., 2021). As mentioned before, the growth of large crystals by aggregation of amorphous particles is a non-classical crystallization pathway, which has been observed and discussed in recent literature (De Yoreo et al., 2015; Banfield et al., 2000). As shown in Table 1A, 'Eerbeek' sludge has a higher selenite bio-reduction rate than 'Emmtec' sludge, producing more amorphous Se^0 in a shorter period, providing a longer reaction time for the aging and crystallization process to large hexagonal crystals.

In the experiments with bio-S^0 large quantities of crystals were found, but these crystals had smaller sizes than for the non-S^0 addition in 'Eerbeek' assays. Only a limited number of larger particles was observed in the SEM picture as bulk crystals. As discussed above, crystalline Se^0 would be produced from amorphous SeS_2 by sulfur bio-reduction. This is a different trajectory for Se crystallization, as discussed in Hageman et al., 2017a because this crystalline structure is thermodynamically more stable than the amorphous structure and can only grow to a larger bulk crystal by an oriented attachment process (De Yoreo et al., 2015). The apparent difference in morphology with and without bio-S^0 and the limited sulfide production from bio-S^0 pointed clearly to sulfur bio-cycling, including SeS_2 (Fig. 1). The different pathways for assays with and without bio-S^0 addition might also be supported by the pH differences in 'Eerbeek' assays by day 21 (Table S2A). The pH decreased from pH 7 to ~6.7 in the absence of bio-S^0, while after adding bio-S^0 the pH increased to ~7.4. However, the pH increased in 'Emmtec' assays irrespective of the bio-S^0 addition (there is a minimal difference in pH changes for addition/non-addition of bio-S^0). One may note that buffer solutions are used as the medium to stabilize the pH. An increase in pH to pH> 7.5 could also promote hexagonal selenium formation, in that way bio-S^0 could advance hexagonal Se^0 formation in two ways.

Regarding the final products of selenate bio-reduction at ~pH 7, it has been commonly reported as spherical amorphous Se^0 (Song et al., 2021; Hageman et al., 2017b; Astratinei et al., 2006; Staicu et al., 2015; Lenz et al., 2008b; Mal et al., 2017). The introduction of bio-S^0 and sulfur bio-cycling (Fig. 1) in this process would allow the production of crystals at pH ~7 by the reduction of the formed intermediate (SeS_2) (Hageman et al., 2017a) or by the crystallization of the bio-produced amorphous Se^0-solids. Compared to the selenite reduction rate (Table 1A) the sulfur's involvement in such a pathway for Se^0 formation from selenate seemed limited as can be concluded from the specific selenate reduction rate (Table 1B). The product for 'Emmtec' with bio-S^0 addition shows relatively more amorphous selenium than for 'Eerbeek', because Se^0 formation from the direct bio-reduction of selenate is relatively more dominant than the chemical pathway as bio-S^0 only resulted in an overall minimal increase and initially even slight negative effect on selenate bio-reduction. For Eerbeek the relative contribution of bio-S^0 reduction and bio-cycling in selenate reduction was higher (Table 1B) and hence a more crystalline Se product was observed.

Table 1A
The specific selenite reduction rate of 'Emmtec' sludge or 'Eerbeek' sludge at day 7 with and without the addition of sulfur species. Conditions of selenite experiments: 1.2 g_{VSS}/L 'Emmtec' or 'Eerbeek' sludge, 30 °C, pH 7, initial selenite concentration: 1.73, 1.99 or 2.2 mmol L^{-1}, using 1.25 mmol L^{-1} lactic acid as electron donor, 0 or 1.12 mmol L^{-1} sulfate or 0, 1, 2, 4 mmol L^{-1} bio-S^0.

Specific selenite reduction rate (mmol Se g^{-1}_{VSS} day^{-1})	No S added	Added bio-S^0	Added SO_4^{2-}
'Emmtec'-selenite	0.087	0.11 ± 0.009[b]	0.17
'Eerbeek'-selenite[a]	0.18	0.21 ± 0.006[c]	n.a.

[a] Experimental data were not shown in this manuscript
[b] The average rate of batch assays with 1, 2, and 4 mmol L^{-1} bio-S^0
[c] The average rate of batch assays with 1 and 4 mmol L^{-1} bio-S^0

Table 1B
The specific selenate reduction rate of 'Emmtec' sludge or 'Eerbeek' sludge at day 28 with and without the addition of 1 mmol $L^{-1}$of sulfur species. Conditions of selenate experiments: 1.2, 2.8, or 5.6 g_{VSS} L^{-1} 'Emmtec' or 'Eerbeek' sludge, 30 °C, pH 7, initial selenate concentration: 1.96 mmol L^{-1}; using 1.25 mmol L^{-1} lactic acid as electron donor, 0, 1, 2, 4 mmol L^{-1} bio-S^0.

Specific selenate reduction rate (mmol Se g^{-1}_{VSS} day^{-1})	No S added	Added bio-S^0
1.2 g^{-1}_{VSS} 'Emmtec'	0.0087	0.0090 ± 0.0015[4])
2.8 g^{-1}_{VSS} 'Emmtec'	0.0074	0.0080
5.6 g^{-1}_{VSS} 'Emmtec'	0.010	0.010 ± 0.0001[4])
5.6 g^{-1}_{VSS} 'Eerbeek'	0.002	0.003 ± 0.0002[4])

[4])The average rate of batch assays with 2, 4 mmol L^{-1} bio-S^0

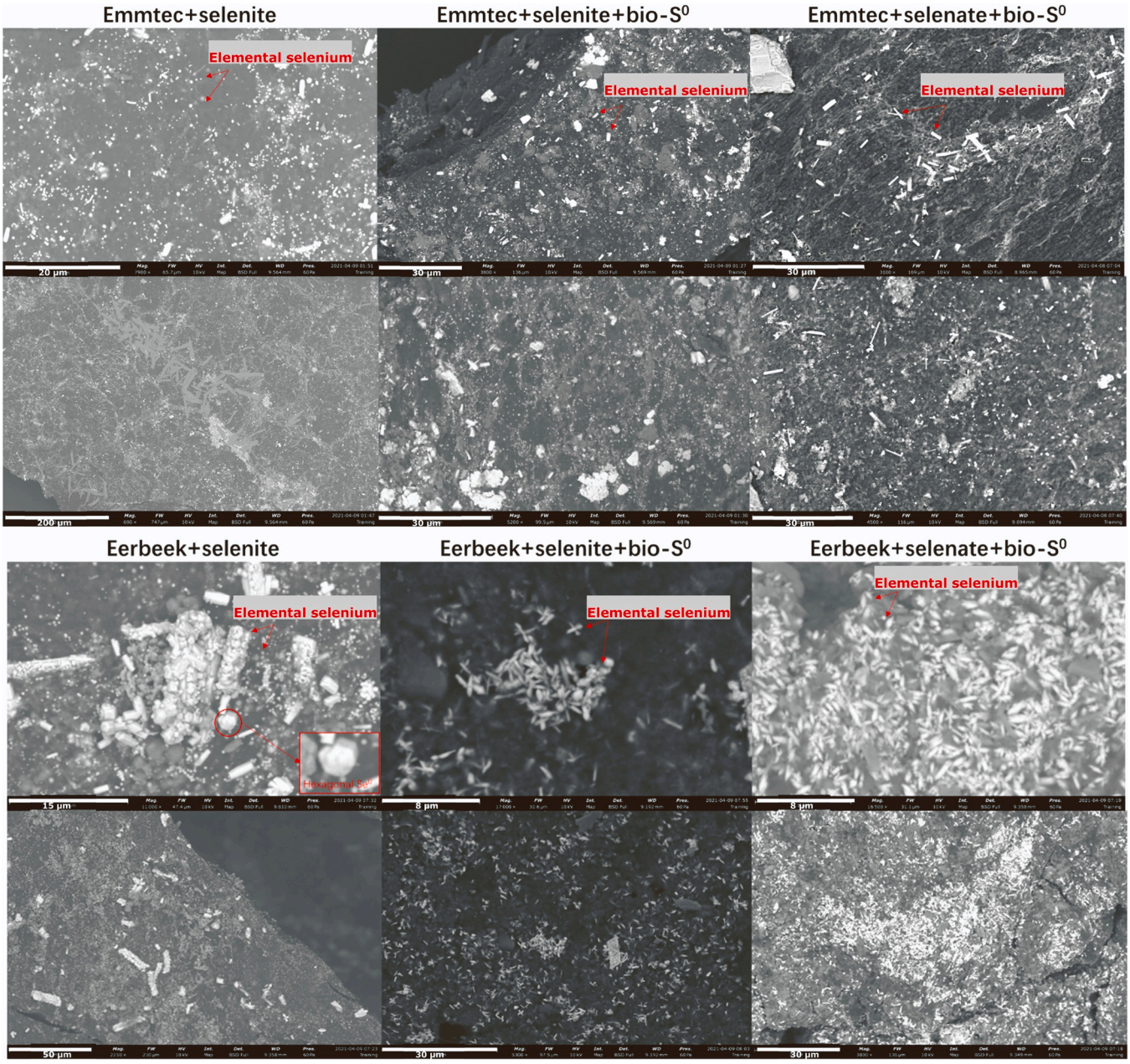

Fig. 8. Evaluation and characterization of the solids sampled from the batch assays on day 20 (for selenite experiments) and day 28 (for selenate experiments), respectively. Acicular-like solid or spherical particles were distinguished by SEM image, and the chemical composition of the selected area was analyzed by EDX (Figure not shown here) confirmed these solids consisted of 100% selenium. Conditions: selenite assays-1.2 g_{VSS} L^{-1} 'Emmtec'/'Eerbeek' sludge, 30 °C, pH 7, initial selenite concentration: 1.92 mmol L^{-1}, using 1.25 mmol L^{-1} lactic acid as electron donor, 0 or 2 mmol L^{-1} bio-S^0; selenate assays-5.6 g_{VSS} L^{-1} 'Emmtec'/'Eerbeek' sludge, 30 °C, pH 7, initial selenate concentration:1.96 mmol L^{-1}, using 1.25 mmol L^{-1} lactic acid as electron donor, 2 mmol L^{-1} bio-S^0.

3.9. Implications for selenium mobility and removal

We found a positive effect of adding bio-S^0 on the crystallinity of the produced Se^0 from selenite bio-reduction for 'Emmtec' and 'Eerbeek'. The biomineralized crystalline black Se^0 with the help of sulfur bio-cycling is hydrophobic and thermodynamically the most stable phase concerning oxidation and could be a way in which the mobility of toxic Se in the environment is reduced. However, this depends on the bacterial consortia present and their relative affinity for all sulfur and selenium species.

The interaction between Se and S can positively influence the reduction rate and the morphology of the final produced Se^0. The involvement of SeS_2 produced from selenite and sulfide in the S-cycling (Fig. 1) was discussed, which may provide an idea of optimizing the selenate bio-reduction process in the future. Bio-S^0 reduction uses less electron donor than sulfate bio-reduction. Elemental sulfur is commonly present in nature and it can spontaneously form by physical SeS_2 dissociation into Se^0 and S^0 (Hockin and Gadd, 2006) during selenium bio-reduction in the presence of sulfur species. Although the bio-S^0 reduction rate is lower than for sulfate, because of bio-availability limitations of it being a solid, it is still an option to apply bio-S^0 in the removal of Se from water in a two-reactor system where first selenate is reduced to selenite, and next selenite is reduced by sulfide formation from bio-cycling resulting in crystalline Se^0 crystals. When the pH is set higher, between 7 and 8, the slightly higher formation of polysulfides can reduce this physical limitation. Apart from improving the removal rate, bio-S^0 addition can also promote hexagonal Se^0 formation (Gebreeyessus and Zewge, 2019).

The involvement of S compounds in the selenate reduction via indirectly reducing selenite by producing sulfide could also help understand the presence of Se^0 in nature, which was suggested to contribute to the presence of elemental selenium in the surface sediments of the Kesterson National Refuge (Hockin and Gadd, 2003; Oremland et al., 1989).

4. Conclusion

The biological cycling of sulfur and selenium when both are present is intertwined. This study found that sulfur's presence as bio-S^0 enhances selenite removal for two different microbial consortia, 'Emmtec' and 'Eerbeek'. The bacterial generation of sulfide from sulfur can chemically react with selenite to form SeS_2, which can be further bio-reduced to black crystalline elemental selenium and sulfide. Biological sulfur-cycling can reduce toxic selenite mobility in the environment by producing hydrophobic and thermodynamically stable crystalline selenium. The prominence of sulfide in solution only after selenite has been reduced indicates SeS_2 reduction and that sulfur cycling indeed can take place. The addition of sulfur also promoted the particles' color and appearance change from red amorphous to black hexagonal elemental selenium. The Se^0 crystalline product from non-classical crystallization and aging was different from the product formed from S-cycling via SeS_2.

Acceleration effects on selenate reduction rate by bio-S^0 addition were seen to a limited degree for 'Eerbeek', but the increase in rate was not as significant as in selenite reduction experiments. For 'Emmtec', the effects of adding bio-S^0 were minimal for selenate reduction. Selenite formation from selenate bio-reduction at the cell and a further immediate reduction might hinder sulfur's involvement from achieving the reaction route demonstrated in Fig. 1. In this sense, by optimization of the process for producing the selenite intermediate from selenate reduction (as we found in our previous research, (Song et al., 2021), then sulfur's bio-cycling can be used as a significant post-treatment to remove selenium to ultra-low concentrations and recover the produced selenium. In nature, selenate being co-present with sulfur species may inhibit selenate bio-reduction for some bacterial species, which may influence the cycling of selenium and sulfur in soil and water. The sulfur-cycling may also change the morphology of the final Se-product, accelerating the mineralization of hexagonal Se^0.

CRediT authorship contribution statement

Bingnan Song: Conceptualization, Investigation, Methodology, Data curation, Writing – original draft preparation, Writing – review & editing, Visualization, Investigation. **Renata van der Weijden**: Funding acquisition, Investigation, Writing – original draft preparation, Writing – review & editing Supervision, Resources. **Jan Weijma**: Funding acquisition, Project administration, Writing – original draft preparation. **Cees Buisman:** Supervision, Writing – review & editing.

Declaration of Competing Interest

The authors declare that they have no known competing financial interests or personal relationships that could have appeared to influence the work reported in this paper.

Data availability

Data will be made available on request.

Acknowledgments

Funding: This work was supported by The Enterprise Agency's Knowledge, Technology and Innovation program (TKI), the Netherlands, within the project Biocrystallization of Selenium down to ultra-low levels, with number 2016WUR003, and the student was supported by the China Scholarship Council.

Novelty statement

This manuscript points to directions for removal of toxic selenium oxyanions as the most stable Se phase. The sulfur species interaction play a role when those are present together with the selenium oxyanions, which is usually the case. In a previously published paper in the Journal of Hazardous materials, the bio-reduction of selenium oxyanions, simulating a waste stream without sulfur species present, was subsequently chemically treated with sodiumsulfide. But here we show that in one step the same is possible by the bio-cycling of sulfur species when both sulfur and selenium are (naturally) present.

Appendix A. Supporting information

Supplementary data associated with this article can be found in the online version at doi:10.1016/j.jhazmat.2022.129367.

References

Alivisatos, A.P., 2000. Naturally aligned nanocrystals. Science (1979) 289, 736–737. https://doi.org/10.1126/science.289.5480.736.

Astratinei, V., Van Hullebusch, E., Lens, P., 2006. Bioconversion of selenate in methanogenic anaerobic granular sludge. J. Environ. Qual. 35, 1873–1883. https://doi.org/10.2134/jeq2005.0443.

Banfield, J.F., Welch, S.A., Zhang, H., Ebert, T.T., Penn, R.L., 2000. Aggregation-based crystal growth and microstructure development in natural iron oxyhydroxide biomineralization products. Science (1979) 289, 751–754. https://doi.org/10.1126/science.289.5480.751.

Chen, K.Y., Gupta, S.K., 1973. Formation of polysulfides in aqueous solution. Environ. Lett. 4, 187–200. https://doi.org/10.1080/00139307309436596.

D'Abzac, P., Bordas, F., Joussein, E., van Hullebusch, E., Lens, P.N.L., Guibaud, G., d'Abzac, P., Bordas, F., Joussein, E., van Hullebusch, E., Lens, P.N.L., Guibaud, G., 2010. Characterization of the mineral fraction associated to extracellular polymeric substances (EPS) in anaerobic granular sludges. Environ. Sci. Technol. 44, 412–418. https://doi.org/10.1021/es901912g.

De Yoreo, J.J., Gilbert, P.U.P.A., Sommerdijk, N.A.J.M., Penn, R.L., Whitelam, S., Joester, D., Zhang, H., Rimer, J.D., Navrotsky, A., Banfield, J.F., Wallace, A.F., Michel, F.M., Meldrum, F.C., Cölfen, H., Dove, P.M., 2015. Crystallization by particle attachment in synthetic, biogenic, and geologic environments. Science 349, aaa6760-1–aaa6760-9. https://doi.org/10.1126/science.aaa6760.

Gebreeyessus, G.D., Zewge, F., 2019. A review on environmental selenium issues. SN Appl. Sci. 1, 1–19. https://doi.org/10.1007/s42452-018-0032-9.

Geoffroy, N., Demopoulos, G.P., 2011. The elimination of selenium(IV) from aqueous solution by precipitation with sodium sulfide. J. Hazard. Mater. 185, 148–154. https://doi.org/10.1016/j.jhazmat.2010.09.009.

Gibson, B.D., Blowes, D.W., Lindsay, M.B.J.J., Ptacek, C.J., 2012. Mechanistic investigations of Se(VI) treatment in anoxic groundwater using granular iron and organic carbon: An EXAFS study. J. Hazard. Mater. 241, 92–100. https://doi.org/10.1016/j.jhazmat.2012.09.015.

Gonzalez-Gil, G., Lens, P.N.L., Saikaly, P.E., 2016. Selenite reduction by anaerobic microbial aggregates: microbial community structure, and proteins associated to the produced selenium spheres. Front. Microbiol. 7, 571. https://doi.org/10.3389/fmicb.2016.00571.

Hageman, S.P.W., van der Weijden, R.D., Weijma, J., Buisman, C.J.N., 2013. Microbiological selenate to selenite conversion for selenium removal. Water Res. 47, 2118–2128. https://doi.org/10.1016/j.watres.2013.01.012.

Hageman, S.P.W., van der Weijden, R.D., Stams, A.J.M., van Cappellen, P., Buisman, C.J.N., 2017a. Microbial selenium sulfide reduction for selenium recovery from wastewater. J. Hazard. Mater. 329, 110–119. https://doi.org/10.1016/j.jhazmat.2016.12.061.

Hageman, S.P.W., van der Weijden, R.D., Stams, A.J.M., Buisman, C.J.N., 2017b. Bio-production of selenium nanoparticles with diverse physical properties for recovery from water. Int. J. Miner. Process. 169, 7–15. https://doi.org/10.1016/j.minpro.2017.09.018.

Hidalgo-Ulloa, A., Sánchez-Andrea, I., Buisman, C., Weijma, J., 2020. Sulfur reduction at hyperthermoacidophilic conditions with mesophilic anaerobic sludge as the inoculum. Environ. Sci. Technol. 54, 14656–14663. https://doi.org/10.1021/acs.est.0c02557.

Hockin, S., Gadd, G.M., 2006. Removal of selenate from sulfate-containing media by sulfate-reducing bacterial biofilms. Environ. Microbiol. 8, 816–826. https://doi.org/10.1111/j.1462-2920.2005.00967.x.

Hockin, S.L., Gadd, G.M., 2003. Linked redox precipitation of sulfur and selenium under anaerobic conditions by sulfate-reducing bacterial biofilms. Appl. Environ. Microbiol 69, 7063–7072. https://doi.org/10.1128/AEM.69.12.7063-7072.2003.

Huang, S.W., Wang, Y., Tang, C., Jia, H.L., Wu, L., 2021. Speeding up selenite bioremediation using the highly selenite-tolerant strain *Providencia rettgeri HF16*-A novel mechanism of selenite reduction based on proteomic analysis. J. Hazard. Mater. 406 https://doi.org/10.1016/j.jhazmat.2020.124690.

Jung, B., Safan, A., Batchelor, B., Abdel-Wahab, A., 2016. Spectroscopic study of Se(IV) removal from water by reductive precipitation using sulfide. Chemosphere 163, 351–358. https://doi.org/10.1016/j.chemosphere.2016.08.024.

M. Kashiwa, S. Nishimoto, K. Takahashi, M. Ike, M. Fujita, M. Ike, M. Fujita, Factors affecting soluble selenium removal by a selenate-reducing bacterium *Bacillus sp. SF-1*, 2000. 89(6) 528–533. https://doi.org/10.1016/S1389–1723(00)80051–1.

Kharma, A., Grman, M., Misak, A., Domínguez-Álvarez, E., Nasim, M.J., Ondrias, K., Chovanec, M., Jacob, C., 2019. Inorganic polysulfides and related reactive sulfur selenium species from the perspective of chemistry. Molecules 24, 1359. https://doi.org/10.3390/molecules24071359.

Lemly, A.D., 2014. An urgent need for an EPA standard for disposal of coal ash. Environ. Pollut. 191, 253–255. https://doi.org/10.1016/J.ENVPOL.2014.04.029.

Lenz, M., Lens, P.N.L., 2009. The essential toxin: the changing perception of selenium in environmental sciences. Sci. Total Environ. 407, 3620–3633. https://doi.org/10.1016/J.SCITOTENV.2008.07.056.

Lenz, M., Van Hullebusch, E.D.V., Hommes, G., Corvini, P.F.X., Lens, P.N.L., 2008a. Selenate removal in methanogenic and sulfate-reducing upflow anaerobic sludge bed reactors. Water Res. 42, 2184–2194. https://doi.org/10.1016/j.watres.2007.11.031.

Lenz, M., Smit, M., Binder, P., van Aelst, A.C., Lens, P.N.L., 2008b. Biological alkylation and colloid formation of selenium in methanogenic UASB reactors. J. Environ. Qual. 37, 1691–1700. https://doi.org/10.2134/jeq2007.0630.

Lortie, L., Gould, W.D., Rajan, S., McCready, R.G.L., Cheng, K.-J., 1992. Reduction of selenate and selenite to elemental selenium by a pse*udomonas stutzeri Isolate,*. Appl. Environ. Microbiol. 58, 4042–4044. https://doi.org/10.1128/aem.58.12.4042-4044.1992.

Lu, J., Fu, F., Ding, Z., Li, N., Tang, B., 2017. Removal mechanism of selenite by Fe_3O4-precipitated mesoporous magnetic carbon microspheres. J. Hazard. Mater. 330, 93–104. https://doi.org/10.1016/j.jhazmat.2017.01.056.

Mal, J., Nancharaiah, Y.V., van Hullebusch, E.D., Lens, P.N.L., 2017. Biological removal of selenate and ammonium by activated sludge in a sequencing batch reactor. Bioresour. Technol. 229, 11–19. https://doi.org/10.1016/j.biortech.2016.12.112.

Millero, F.J., 1986. The thermodynamics and kinetics of the hydrogen sulfide system in natural waters. Mar. Chem. 18, 121–147. https://doi.org/10.1016/0304-4203(86)90003-4.

Minaev, V.S., Timoshenkov, S.P., Kalugin, V.V., 2005. Structural and phase transformations in condensed selenium. J. Optoelectron. Adv. Mater. 7, 1717–1741.

Ojeda, J.J., Merroun, M.L., Tugarova, A. v, Lampis, S., Kamnev, A.A., Gardiner, P.H.E., 2020. Developments in the study and applications of bacterial transformations of selenium species. Crit. Rev. Biotechnol. 40, 1250–1264. https://doi.org/10.1080/07388551.2020.1811199.

Ontiveros-Valencia, A., Penton, C.R., Krajmalnik-Brown, R., Rittmann, B.E., 2016. Hydrogen-fed biofilm reactors reducing selenate and sulfate: community structure and capture of elemental selenium within the biofilm. Biotechnol. Bioeng. 113, 1736–1744. https://doi.org/10.1002/bit.25945.

Oremland, R.S., Hollibaugh, J.T., Maest, A.S., Presser, T.S., Miller, L.G., Culbertson, C. W., 1989. Selenate reduction to elemental selenium by anaerobic bacteria in sediments and culture: biogeochemical significance of a novel, sulfate-independent respiration. Appl. Environ. Microbiol. 55, 2333–2343. https://doi.org/10.1128/aem.55.9.2333-2343.1989.

Pettine, M., Gennari, F., Campanella, L., Casentini, B., Marani, D., 2012. The reduction of selenium(IV) by hydrogen sulfide in aqueous solutions. Geochim. Et. Cosmochim. Acta 83, 37–47. https://doi.org/10.1016/j.gca.2011.12.024.

Piacenza, E., Presentato, A., Ferrante, F., Cavallaro, G., Alduina, R., Martino, D.F.C., 2021. Biogenic selenium nanoparticles: a fine characterization to unveil their thermodynamic stability. Nanomaterials 11. https://doi.org/10.3390/nano11051195.

Rayman, M.P., 2012. Selenium and human health. Lancet 379, 1256–1268. https://doi.org/10.1016/S0140-6736(11)61452-9.

Song, B., Tian, Z., van der Weijden, R.D., Buisman, C.J.N., Weijma, J., 2021. High-rate biological selenate reduction in a sequencing batch reactor for recovery of hexagonal selenium. Water Res. 193, 116855 https://doi.org/10.1016/J.WATRES.2021.116855.

Staicu, L.C., Van Hullebusch, E.D., Oturan, M.A., Ackerson, C.J., Lens, P.N.L.L., 2015. Removal of colloidal biogenic selenium from wastewater. Chemosphere 125, 130–138. https://doi.org/10.1016/j.chemosphere.2014.12.018.

Stams, A.J.M., Grolle, K.C.F., Frijters, C.T.M.J., Van Lier, J.B., 1992. Enrichment of thermophilic propionate-oxidizing bacteria in syntrophy with *Methanobacterium thermoautotrophicum* or *Methanobacterium thermoformicicum*. Appl. Environ. Microbiol. 58, 346–352.

Steinberg, N.A., Oremland, R.S., 1990. Dissimilatory selenate reduction potentials in a diversity of sediment types. Appl. Environ. Microbiol. 56, 3550–3557. https://doi.org/10.1128/aem.56.11.3550-3557.1990.

Tan, L.C., 2018. Anaerobic treatment of mine wastewater for the removal of selenate and its co-contaminants. CRC Press. https://doi.org/10.1201/9780429448676.

Tan, L.C., Nancharaiah, Y.V., van Hullebusch, E.D., Lens, P.N.L., 2016. Selenium: environmental significance, pollution, and biological treatment technologies. Biotechnol. Adv. 34, 886–907. https://doi.org/10.1016/j.biotechadv.2016.05.005.

Tan, L.C., Espinosa-Ortiz, E.J., Nancharaiah, Y.V., van Hullebusch, E.D., Gerlach, R., Lens, P.N.L., 2018a. Selenate removal in biofilm systems: effect of nitrate and sulfate on selenium removal efficiency, biofilm structure and microbial community. J. Chem. Technol. Biotechnol. 93, 2380–2389. https://doi.org/10.1002/jctb.5586.

Tan, Y., Wang, Y., Wang, Y., Xu, D., Huang, Y., Wang, D., Wang, G., Rensing, C., Zheng, S., 2018b. Novel mechanisms of selenate and selenite reduction in the obligate aerobic bacterium Comamonas testosteroni S44. J. Hazard. Mater. 359, 129–138. https://doi.org/10.1016/J.JHAZMAT.2018.07.014.

Ullah, H., Liu, G., Yousaf, B., Ali, M.U., Abbas, Q., Munir, M.A.M., Mian, M.M., 2018. Developmental selenium exposure and health risk in daily foodstuffs: a systematic review and meta-analysis. Ecotoxicol. Environ. Saf. 149, 291–306. https://doi.org/10.1016/J.ECOENV.2017.11.056.

Valdiglesias, V., Pásaro, E., Méndez, J., Laffon, B., 2010. In vitro evaluation of selenium genotoxic, cytotoxic, and protective effects: a review. Arch. Toxicol. 84, 337–351. https://doi.org/10.1007/s00204-009-0505-0.

Vogel, M., Fischer, S., Maffert, A., Hübner, R., Scheinost, A.C., Franzen, C., Steudtner, R., 2018. Biotransformation and detoxification of selenite by microbial biogenesis of selenium-sulfur nanoparticles. J. Hazard. Mater. 344, 749–757. https://doi.org/10.1016/j.jhazmat.2017.10.034.

Wang, D., Rensing, C., Zheng, S., 2022. Microbial reduction and resistance to selenium: Mechanisms, applications and prospects. J. Hazard. Mater. 421, 126684 https://doi.org/10.1016/J.JHAZMAT.2021.126684.

White, P.J., Broadley, M.R., Bowen, H.C., Johnson, S.E., 2007. Selenium and its relationship with sulfur. In: Selenium and its relationship with sulfur. Springer, Dordrecht, pp. 225–252. https://doi.org/10.1007/978-1-4020-5887-5_10.

Yee, N., 2011. Geomicrobiology of selenium: life and death by selenite. Appl. Geochem. 26, 324–325. https://doi.org/10.1016/J.APGEOCHEM.2011.03.077.

Zambonino, M.C., Quizhpe, E.M., Jaramillo, F.E., Rahman, A., Vispo, N.S., Jeffryes, C., Dahoumane, S.A., 2021. Green synthesis of selenium and tellurium nanoparticles: Current trends, biological properties and biomedical applications. Int. J. Mol. Sci. 22, 1–34. https://doi.org/10.3390/ijms22030989.

Zehr, J.P., Oremland, R.S., 1987. Reduction of selenate to selenide by sulfate-respiring bacteria: experiments with cell suspensions and estuarine sediments. Appl. Environ. Microbiol. 53, 1365–1369. https://doi.org/10.1016/0198-0254(87)96089-4.

Zoroufchi Benis, K., McPhedran, K.N., Soltan, J., 2022. Selenium removal from water using adsorbents: a critical review. J. Hazard. Mater. 424 (Part C), 127603 https://doi.org/10.1016/J.JHAZMAT.2021.127603.